Journal of the Brazilian Society of Mechanical Sciences and Engineering (2020) 42:369
https://doi.org/10.1007/s40430-020-02438-8

TECHNICAL PAPER

Vibration, tool wear and surface roughness characteristics in turning of Inconel 718 alloy with ceramic insert under LN_2 machining

Wenping Mou[1] · **Shaowei Zhu**[2]

Received: 13 July 2019 / Accepted: 28 May 2020 / Published online: 16 June 2020

Abstract

Liquid nitrogen (LN_2) machining is considered as a safe, clean, and environmentally friendly machining process. This paper aims to investigate the vibration, tool wear and surface roughness mechanism of the ceramic insert during turning of Inconel 718 alloy under dry machining and LN_2 machining. The experiments were performed at three cutting speeds (100, 150, 200 m/min), feed rates (0.04, 0.08, 0.12 mm/rev) and depths of cut (0.2, 0.4, 0.6 mm). The experiment results show better machinability and longer tool life in LN_2 machining. The vibration acceleration is reduced by 14–32%. A 17–34% reduction of workpiece surface roughness is observed. Flank wear and notch are the predominant wear forms both in LN_2 machining and dry machining, and 16–34% reduction of flank wear is noted in LN_2 machining.

Keywords Liquid nitrogen · Inconel 718 alloy · Ceramic insert · Vibration · Tool wear

1 Introduction

Inconel 718, which has a variety of engineering advantages such as excellent heat resistance, corrosion resistance, ductility, creep, and fatigue properties, is commonly used in high-temperature applications such as automotive, aerospace industry and nuclear reactor [1]. However, Inconel 718 alloy is difficult to machine due to its poor machinability characteristic such as low thermal conductivity. High cutting temperature near the tool–chip interface produces severe edge chipping and plastic deformation, and the tool material is subject to high chemical reactivity, leading to an increase in tool wear and poor surface finish [2, 3]. Conventional coolants fail to reduce the cutting temperature at the tool–chip interface at high cutting speed and feed rate [4, 5]. Further, the cutting fluid disposal is a significant issue, in that an expensive treatment is required before exposing it to the environment [6]. Considering all things, it is essential to shift toward eco-friendly, economic, and green sustainable machining techniques.

Many researchers have used liquid nitrogen LN_2 (− 196 °C) as a cryogenic cooling to reduce the chip–tool interface temperature. Hong and Ding [7] used LN_2 spraying on the machining zone in the turning of Ti–4Al–6V, and observed reductions in the cutting force and coefficient of friction compared with dry machining. LN_2 provides the cushioning effect for the interface surfaces. LN_2 machining improved the turning performance associated with minimum quantity lubrication (MQL) and flood machining conditions even at high cutting speed and feed rate [8]. Venugopal et al. [9] studied experiments on Ti–6Al–4V alloy. They found that the tool life is enhanced in LN_2 machining compared to dry and flood machining. Dhananchezian et al. [10] conducted the AISI 304 turning experiment using a modified cutting insert for facilitate supplying the LN_2 and found that there is a significant reduction in tool wear when compared with the wet environment.

Dhar and Kamruzzaman [11] examined the LN_2 cooling mechanism over a dry environment in the turning of AISI 4037, and significant improvement in surface roughness was noticed. Several researches have focused on LN_2 machining in terms of cutting temperature, cutting force, surface finish,

---

Technical Editor: Adriano Fagali de Souza.

Shaowei Zhu
swjtu_zsw@163.com

Wenping Mou
mouwenp@qq.com

[1] College of Mechanical and Electrical Engineering, Nanjing University of Aeronautics and Astronautics, Nanjing 210016, China

[2] NC Machining Plant, Chengdu Aircraft Industrial (Group) Co., Ltd, Chengdu 610092, China

and tool wear, but there are still minimal papers presenting the vibration analysis in LN_2 machining. To achieve a better surface quality, the workpiece set-up and machine tool should be adequately rigged [12]. Thomas and Beauchamp [13] analyzed the turning vibration when using different machining parameters (cutting speed, feed rate, and depth of cut), different diameters and lengths of the workpieces, and various tool holder lengths and tool nose radius by means of statistical analysis. Typically, vibrations are examined using different sensors, such as dynamometer and accelerometer [14].

Hessainia et al. [15] investigated the surface roughness in cutting of difficult-to-cut materials, evaluated the influence of the machining parameters and vibration. In this work, a strong correlation between feed rate and surface roughness is observed. Abouelatta and Mádl [16] investigated the roughness based on different machining parameters and analysis on tool vibration. It is noted that the feed rate influences the tool vibration.

Ceramic tool materials such as Al_2O_3–TiC mixed ceramics, Si_3N_4 ceramics, sialon, cubic boron nitride (CBN), and SiC whisker-reinforced Al_2O_3 ceramics are progressively used [17] for the turning of Ni-based alloys at a high cutting speed in the range of 120–300 m/min. CBN tool has better capability to resist the notch wear. However, the adhesive wear is a drawback while turning of Inconel 718 alloy [18–20]. For lower notch wear, SiC–Al_2O_3 is better compared with Al_2O_3–TiC inserts, but higher flank wear in the cutting speed range of 100–300 m/min [21]. Altin et al. [22] experimented SiC–Al_2O_3 and sialon tools in the cutting speed range of 150–300 m/min. They found that both the tools have similar flank wear at the optimum cutting speed of around 250 m/min.

Qiang Wang et al. [23] investigated machining characteristics of Inconel 718 by ultrasonic elliptical vibration-assisted turning process. They reported that ultrasonic vibration significantly reduces the cutting force and cutting temperature when compared with the conventional turning process. Sıtkı Akıncıoğlu et al. [24] studied the performance of cryogenically treated (SNMG 120,408) tungsten carbide for turning of Hastelloy C22. They used Taguchi's orthogonal array technique and optimize process parameters. They found that surface roughness was improved by 28.3 and 72.3% by shallow (CT1) cryogenic treatment and deep cryogenic treatment (T2) applied to cementite carbide tools (UT). Çagrı Vakkas Yıldırım et al. [25] used a three different SANDVIK ceramic tools having different structures: Ti[C, N]-mixed alumina inserts (CC650), SiC whisker-reinforced alumina inserts (CC670) and alumina and SiAlON ceramic inserts (CC6060), in the milling of nickel-based waspaloy under dry, wet and MQL processes. As a result of the study, it was observed that the dominant wear type was notch wear, while the most extended tool life was provided with SiAlON-based tools. Çağrı VakkasYıldırım et al. [26] machined Inconel 625 using PVD-TiAlN/TiN coated carbide tools CNGG 120404 (S05–S25). Three different cooling/lubrication strategies were used; these are MQL, cryogenic cooling, and CryoMQL (MQL + LN2). They observed that the tool wear is decreased by 50.67% and 79.60% by the use of MQL and CryoMQL compared with cryogenic machining.

Till now, no one has attempted to understand the vibration characteristics in turning of Inconel 718 alloy using ceramic insert under dry and LN_2 machining. The objective of the present study is to compare the performance characteristics, including vibration acceleration, surface roughness, and tool wear of LN_2 machining with dry machining.

The remainder of this paper is organized as follows. Section 2 presents the set-up and design of the experiment. Section 3 presents the results and discussions of the experiment, including vibration acceleration, surface roughness, and tool wear. Finally, the conclusions are drawn in Sect. 4.

2 Experimental work

2.1 Experimental conditions

The schematic view of the experimental set-up is shown in Fig. 1. The turning process was carried out on a PUMA-2000 CNC lathe at room temperature. The workpiece is 80 mm in diameter and 400 mm in length. The physical properties and chemical composition of the workpiece material Inconel 718 are given in Tables 1 and 2. The whiskers ceramic insert with grade WG 300 and specifications SNGA 120412 are used. The flank tool wear was measured by a Dino-Lite microscope, the ceramic insert is removed after cutting each 140 mm length of the workpiece, and the flank wear value is recorded. A PCB 356A15 acceleration sensor is fixed on the tool holder by a magnetic fixture, and the vibration signal during the turning process is recorded by a NI 9234 data acquisition board. The machined workpiece was degreased using ethanol by ultrasonic cleaning for 10 min. Then a TR200 portable surface roughness tester was used for measuring the roughness of the machined surfaces. Once the average flank wear, $VB_B \geq 0.3$ mm, the microtopography of the flank face, and rake face were observed using a quanta FEG 250 scanning electron microscope (SEM).

2.2 LN_2 cryogenic cooling system

In the present study, a 50-L cryogenic Dewar is used to supply the LN_2. By providing 3 bar pressure into the cryogenic Dewar, the amount of liquid nitrogen comes out via the flexible hose nozzle and sprays into the cutting zone

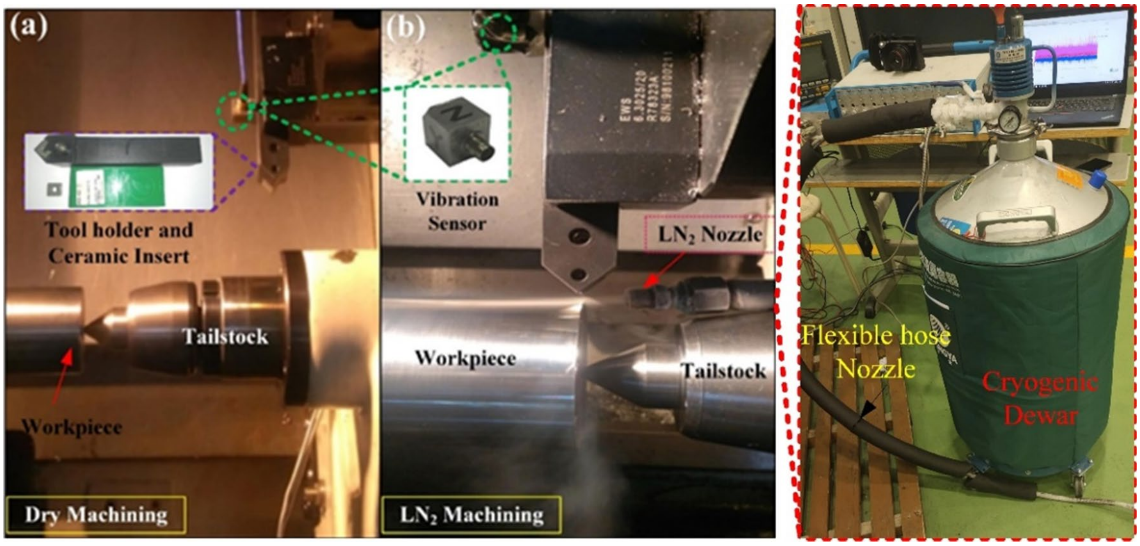

Fig. 1 Experimental set-up. **a** Dry machining, **b** LN_2 machining

Table 1 Physical properties of Inconel 718

Tensile strength (MPa)	Yield strength (MPa)	Elongation (%)	Hardness (HB)
1170	1375	23.3	388

during turning operations. The diameter of the nozzle is 3 mm, the spray angle is 45°, and the spray distance is 45 mm. Figure 2 shows the schematic view of the LN_2 cryogenic cooling system.

Table 3 Factors and levels of the experimental design

Factor	Level 1	Level 2	Level 3
Cutting speed (m/min)	100	150	200
Feed rate (mm/rev)	0.04	0.08	0.12
Depth of cut (mm)	0.2	0.4	0.6

2.3 Experimental design

The turning was carried out under dry and LN_2 cooling environments, respectively. For studying the vibration and the surface roughness, L_{27} full factorial experimental

Table 2 Chemical composition of Inconel 718 (wt %)

Ni	Cr	C	Mn	Si	Co	Mo	Nb	Ti	Al	Fe
53	18	0.04	0.08	0.08	0.23	3.04	5.3	0.98	0.50	17.80

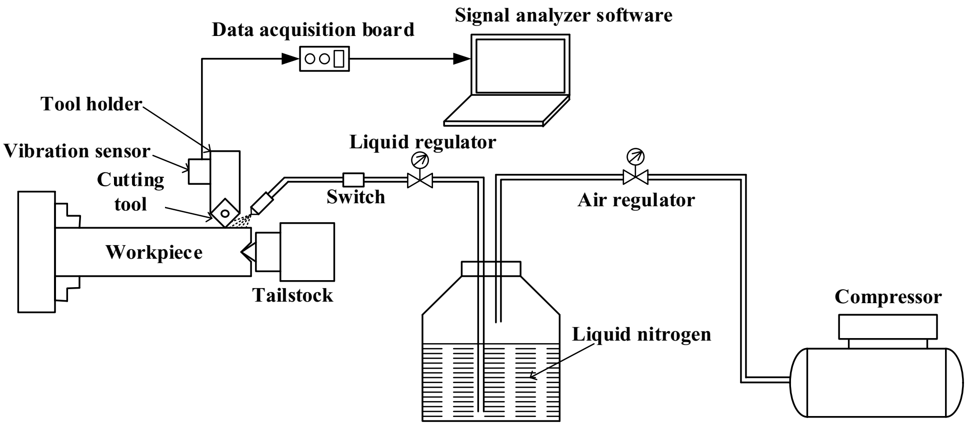

Fig. 2 Schematic view of the LN_2 cryogenic cooling system

design was adopted under each cooling condition. As shown in Table 3, cutting speed (m/min), feed rate (mm/rev), and depth of cut (mm) are selected as experimental factors, and three levels are set for each factor, based on trial experiment and previous literature data. For studying the tool wear, the cutting speed 250 m/min, 300 m/min, and 350 m/min were selected with a constant feed rate 0.1 mm/rev and a constant depth of cut 0.1 mm.

3 Results and discussion

3.1 Vibration acceleration

Figure 3 shows the variations of the vibration acceleration (a_x) vs. feed rate at different cutting speeds and depths of cut (Doc) in the turning of Inconel 718 alloy under dry and LN_2 machining. It can be seen the vibration acceleration varies from 0.244 to 0.772 m/s^2 in dry machining, and from 0.1854 to 0.6723 m/s^2 in LN_2 machining, respectively. In both the cooling conditions, the vibration acceleration grows with the increase of feed rate. For all cutting parameter combinations, the vibration accelerations in LN_2 machining are lower than in dry machining. The maximum vibration acceleration reduction is 32% while the cutting speed is 150 m/min, the feed rate is 0.12 mm, and the depth of cut is 0.2 mm. And the minimum reduction is 14% while the cutting speed is 200 m/min, the feed rate is 0.12 mm, and the depth of cut is 0.6 mm.

Vibration acceleration is directly proportional to the cutting speed and feed rate. Compared with in LN_2 machining, higher cutting speed and feed rate causes more vibration due to noticed aggregation of chips at the machining zone in dry machining, as shown in Fig. 4 [27–29]. Furthermore,

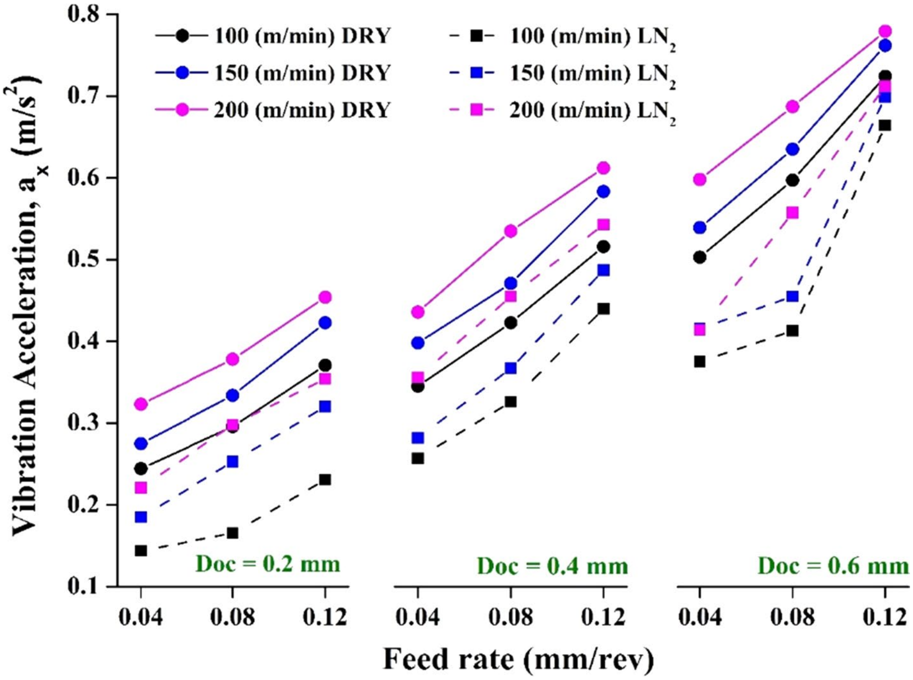

Fig. 3 Variations of the vibration acceleration vs. feed rate at different cutting speed and depth of cut (Doc)


(a) (b)

Fig. 4 Aggregation of chips. **a** Dry machining, **b** LN_2 machining

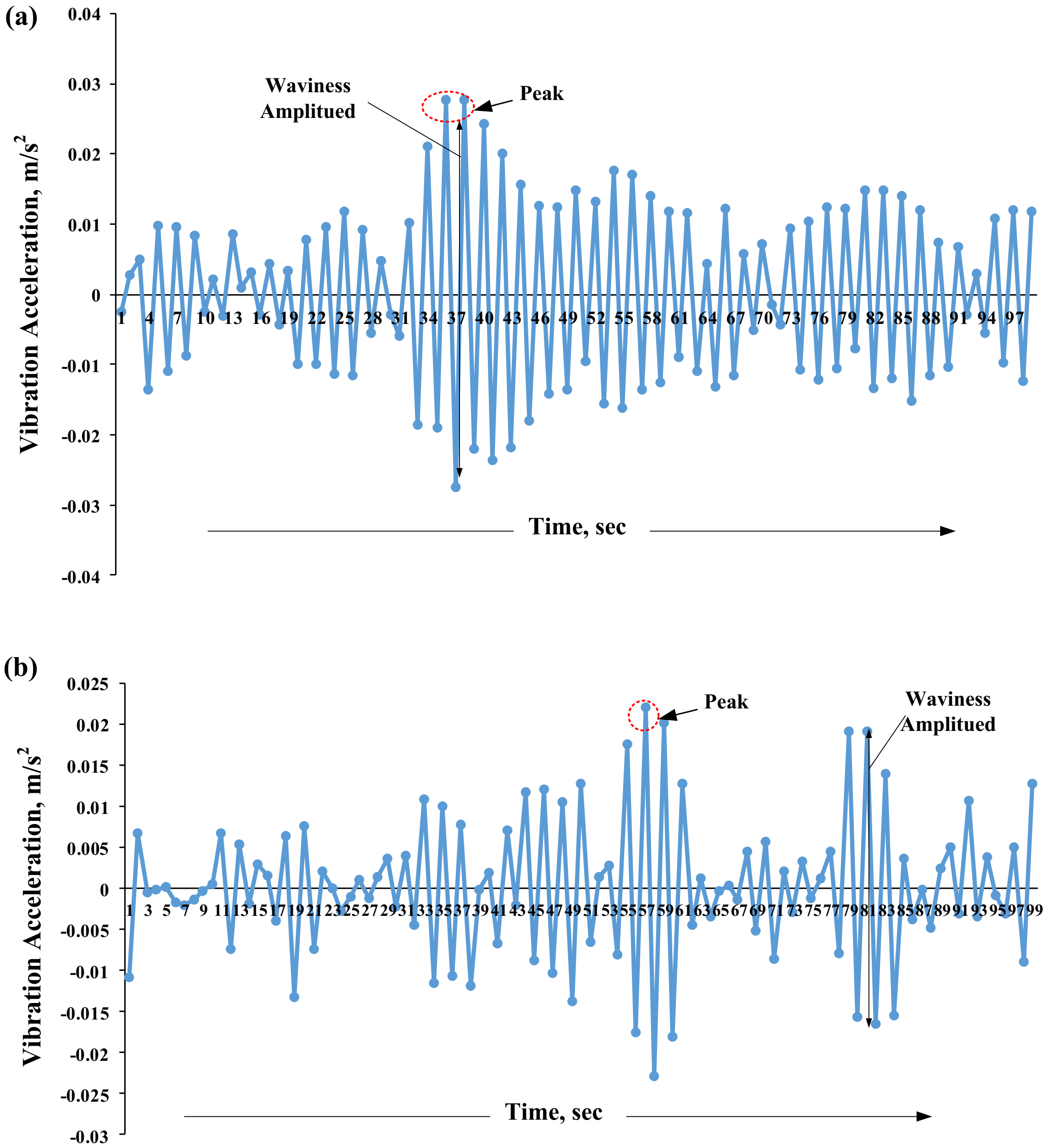

Fig. 5 Vibration acceleration signals while cutting speed is 200 m/min, feed rate is 0.12 mm/rev, and depth of cut is 0.6 mm. **a** Dry machining, **b** LN$_2$ machining

Fig. 5 shows the vibration acceleration signals while the cutting speed is 200 m/min, the feed rate is 0.12 mm/rev, and the depth of cut is 0.6 mm in dry and LN$_2$ machining, respectively. In both the machining conditions, vibration acceleration signals are non-uniform. In dry machining, the vibration peak profile and vibration amplitude are greater, this is due to the tool–chip interface generates higher temperature, and consequently causes the accumulation of chip which leads to affect the machined surface and also reduce the tool life. On the other hand, the vibration peak profile and vibration amplitude is less due to the application of LN$_2$ machining significantly reduces the cutting temperature in the tool–chip interface and reduces the chip accumulation. Therefore, better surface and lighter tool wear were observed in LN$_2$ machining compared with in dry machining. In other words, in LN$_2$ machining, vibration reduction may be attributed to the periodic clearances imposed between the cutting tool and the workpiece in both the feed and radial directions causes less tool wear, chips were no longer wrapped around the workpiece and could be easily broken because of the vibration of cutting tool in the base plane when compared to dry machining. [30].

Fig. 6 Variation of the surface roughness (Ra) vs. feed rate at different cutting speed and depth of cut (Doc)

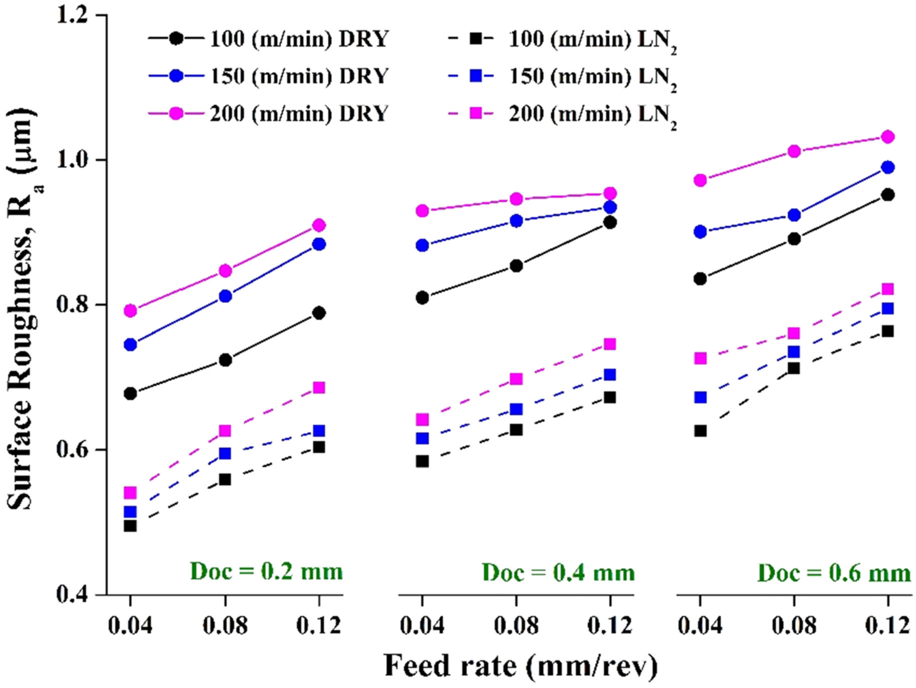

3.2 Surface roughness

Figure 6 shows surface roughness (Ra) vs. feed rate at different cutting speed and depth of cut in the turning of Inconel 718 alloy under dry and LN_2 machining. The surface roughness varies from 0.678 to 1.032 µm in dry machining, and from 0.495 to 0.822 µm in LN_2 machining, respectively. In both the cooling conditions, the surface roughness grows with the increase of the feed and the depth of cut. For all cutting parameter combinations, the surface roughness in LN_2 machining is lower than in dry machining. The maximum surface roughness reduction is 34% while the cutting speed is 200 m/min, the feed rate is 0.04 mm/rev, and the depth of cut is 0.2 mm. And the minimum reduction is 17% while the cutting speed is 100 m/min, the feed rate is 0.08 mm/rev, and the depth of cut is 0.6 mm.

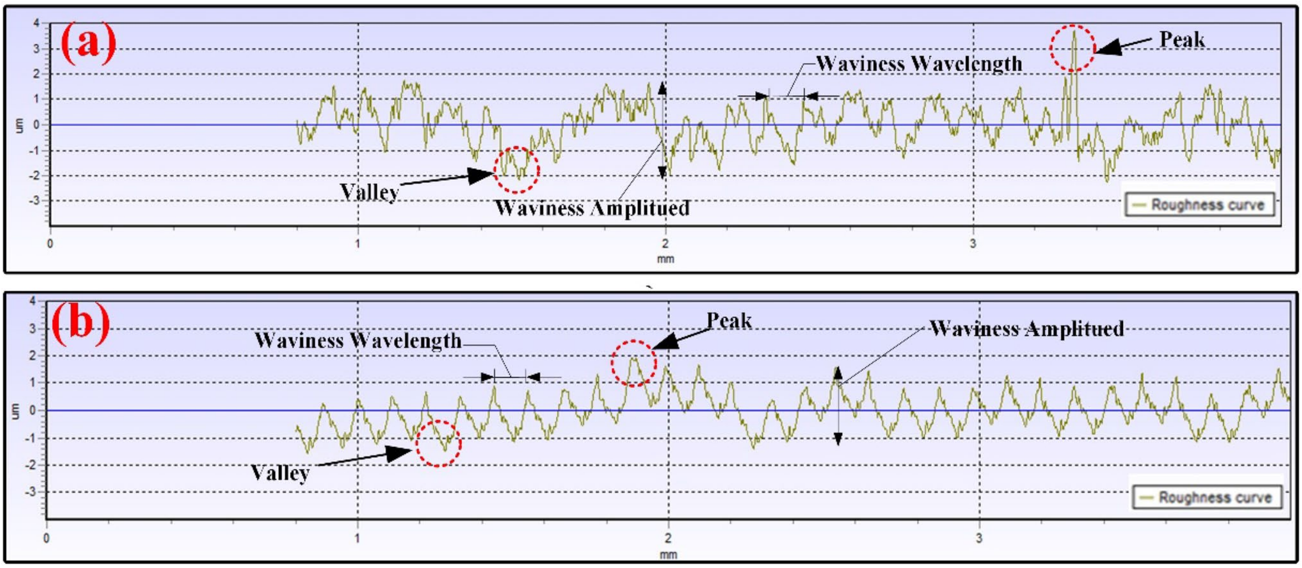

Fig. 7 Workpiece surface roughness while cutting speed is 100 m/min, feed rate is 0.08 mm/rev, and depth of cut is 0.2 mm. **a** Dry machining, **b** LN_2 machining

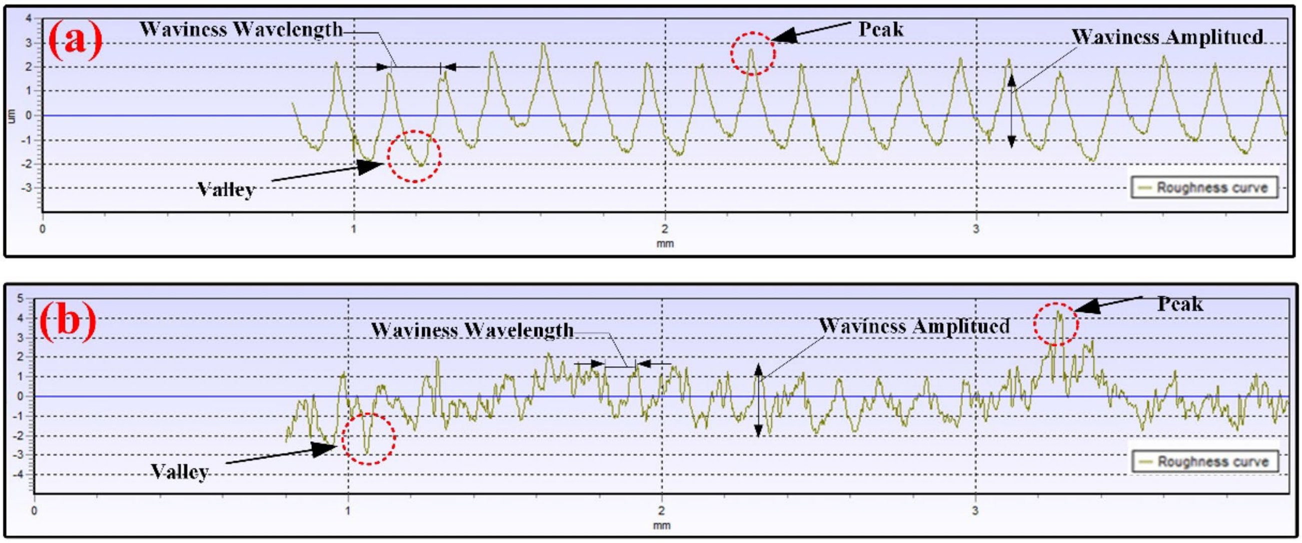

Fig. 8 Workpiece surface roughness while cutting speed is 200 m/min, feed rate is 0.12 mm/rev, and depth of cut is 0.6 mm. **a** Dry machining, **b** LN_2 machining

Figure 7 shows the surface roughness curves in dry and LN_2 machining while the cutting speed is 100 m/min, the feed rate is 0.08 mm/rev, and the depth of cut is 0.2 mm. The roughness profile curves are non-uniform in nature. In the profile curve, average surface roughness is evaluated by peaks, valleys, waviness amplitude, and waviness wavelength. The curves in different cutting speed and feed rate combinations are observed. When using lower cutting speed and feed rate, the roughness curve profile pattern in LN_2 machining is different from that in dry machining. The profile pattern is much regular and uniform in LN_2 machining compared with that in dry machining. For all the cutting parameter combinations, the surface roughness observed in LN_2 machining is lower than that in dry machining [31, 32]. Furthermore, using higher cutting speed and feed rate produces more vibration, which may decrease the workpiece surface roughness when the depth of cut is constant. Figure 8 shows the surface roughness curves in dry and LN_2 machining while the cutting speed is 200 m/min, the feed rate is 0.12 mm/rev, and the depth of cut is 0.6 mm. Both in dry and LN_2 machining, uniform and repeated profile patterns are observed. However, the nature of peaks, valleys, waviness amplitude, and waviness wavelength in dry machining is more significant than that in LN_2 machining. This is due to the lower friction coefficient between the workpiece–tool, favorable chip breakability, and less chip accumulation noticed in the machining zone, which reduces the vibration and improves the surface roughness [33, 34].

3.3 Tool wear

3.3.1 Flank wear

Figure 9 shows the variations of flank wear vs. cutting length (machined workpiece length) in dry and LN_2 machining while the feed rate is 0.1 mm/rev, the depth of cut is 0.1 mm, and the cutting speed is 250 m/min, 300 m/min, and 350 m/min. During the turning process, the tool flank wear is measured once the cutting length reaches 140 mm. When the flank wear reaches 0.3 mm, the tool is considered to achieve its life.

In Fig. 9, it can be seen that the effective cutting length is between 420 and 560 mm in the dry machining, and between 700 and 840 mm in the LN_2 machining. The application of LN_2 cooling results in about 34% longer tool life than in dry machining. The tool wear gradually grows with the increase of cutting length. In the first cutting process (cutting speed is 250 m/min), the flank wear under both cutting conditions are close, and the amount of wear under liquid nitrogen cooling is relatively slow. When the cutting speed increases to 300 m/min, the tool wear grows significantly. But in the third cutting process (cutting speed is 350 m/min), the flank wear under both cutting conditions is close again. When the cutting speed is 250 m/min, 300 m/min, and 350 m/min, the tool flank wear increase by 34%, 27%, and 16% in LN_2 machining compared with that in dry machining. This is because the cooling effect of LN_2 can reduce the cutting temperature and the shear strength of the workpiece material, thus reducing tool wear [35–37].

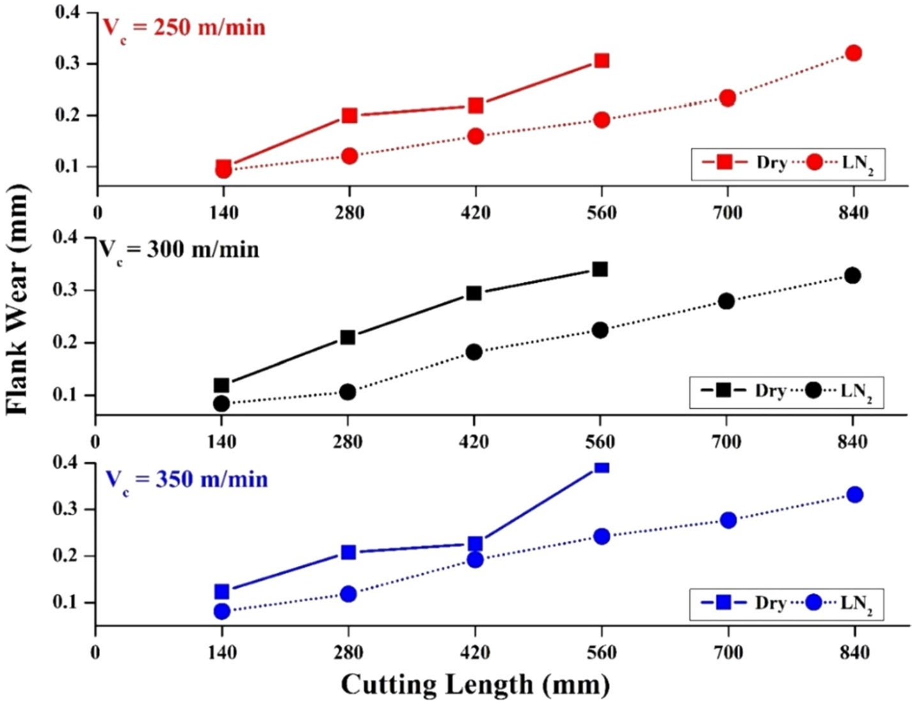

Fig. 9 Variations of the tool flank wear vs. cutting length while the feed rate is 0.1 mm/rev, the depth of cut is 0.1 mm, and the cutting speed is 250 m/min, 300 m/min, and 350 m/min

3.3.2 Flank face microtopography

After reaching the tool life (average flank wear $VB_B \geq 0.3$ mm), the flank surface of the ceramic cutting inserts was observed by using the SEM. Figure 10 shows the SEM images of the inserts' flank face microtopography while the cutting speed is 250 m/min, 300 m/min, and 350 m/min with a constant feed rate 0.1 mm/rev and a constant depth of cut 0.1 mm. The wear mechanism is identified as spilling and mechanical chipping, with less importance diffusion.

As shown in Fig. 10, many abrasion wear marks are observed on flank face. The adhesion wear is found apparently near the tooltip when increasing the cutting speed from 250 m/min to 350 m/min in the dry and LN_2 machining. At the cutting speed of 350 m/min, notch wear is noticed at the end of the cut. It is also found that attrition and chippings are the dominant wear mechanism, with less importance abrasion and diffusion. Compared with in dry machining, in LN_2 machining, the tool flank face microtopography shows less area of diffusion and fracture. The damage is a little smoother because the liquid nitrogen can take away part of the cutting heat, thus leads to more extended tool life [38–40].

3.3.3 Rake face microtopography

After reaching the tool life (average flank wear $VB_B \geq 0.3$ mm), the rake surface microtopography of the ceramic cutting inserts was also observed by using the SEM. Figure 11 shows the SEM images of the insert's rake face microtopography while the cutting speed is 250 m/min, 300 m/min, and 350 m/min with a constant feed rate 0.08 mm/rev and a constant depth of cut 0.1 mm. It can be seen in Fig. 11 that, both in dry and LN_2 machining, the predominant wear type is a notch, with the presence of crater and adhesion. When the cutting speed is 350 m/min, the notch is the predominant wear, which could be found at the end of cut both in dry and LN_2 machining.

The formation of the adhered layer is observed on the tool rake face during the turning of a nickel-based alloy in both the cooling conditions. Abrasive wear marks and workpiece material adhesion are prevalent in both the conditions. Moreover, severe wear patterns such as diffusion and fracture are also observed in the cutting speed range of 300–350 m/min. This phenomenon is attributed to the high strain rate and work hardening, which are characteristic behaviors of nickel alloy, and the heat concentrated at the chip–tool contact area. Compared with in dry machining, less crater wear, adhesion, and notch wear in all cutting parameter combinations are observed in LN_2 machining. This is due to the cushioning effect of LN_2 coolant, and the reduction of cutting temperature in the tool–chip interface consequently enhances the tool life [41–43].

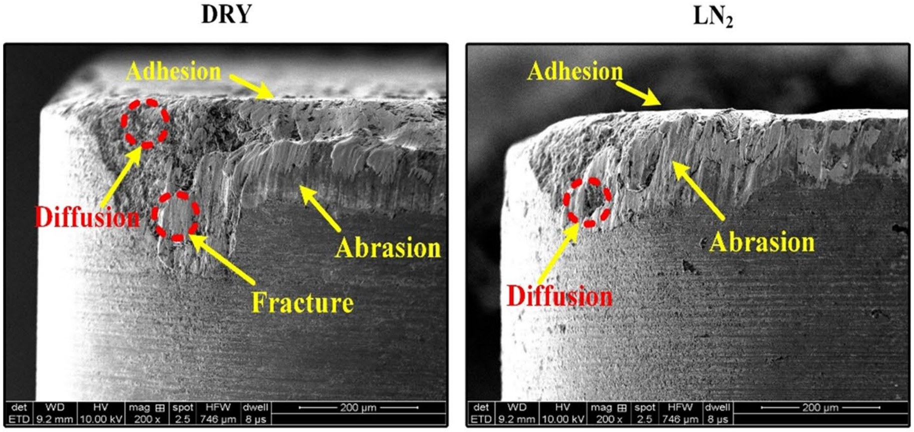

(a) *Vc = 250 m/min*

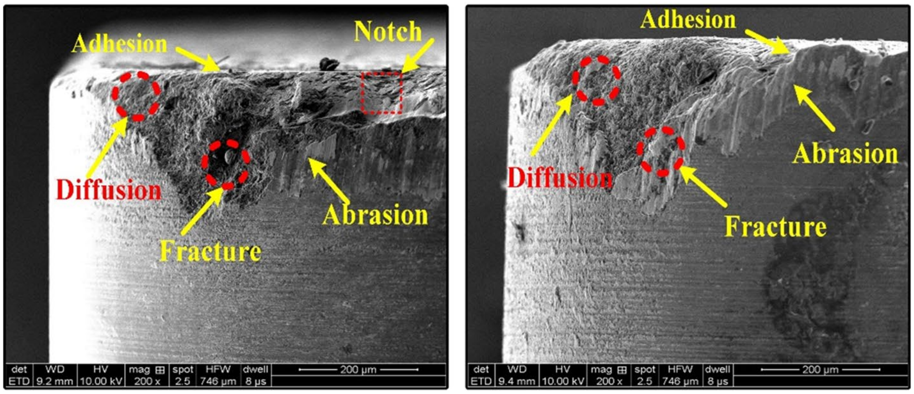

(b) *Vc = 300 m/min*

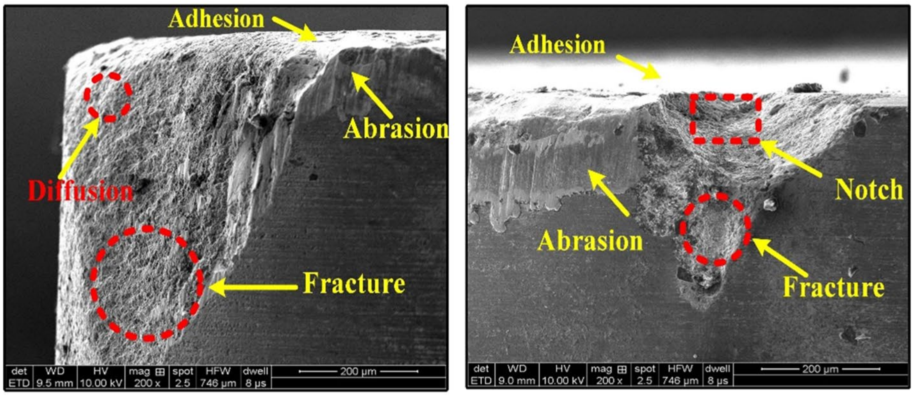

(c) *Vc = 350 m/min*

Fig. 10 SEM images of the flank face after the inserts reaching the tool life

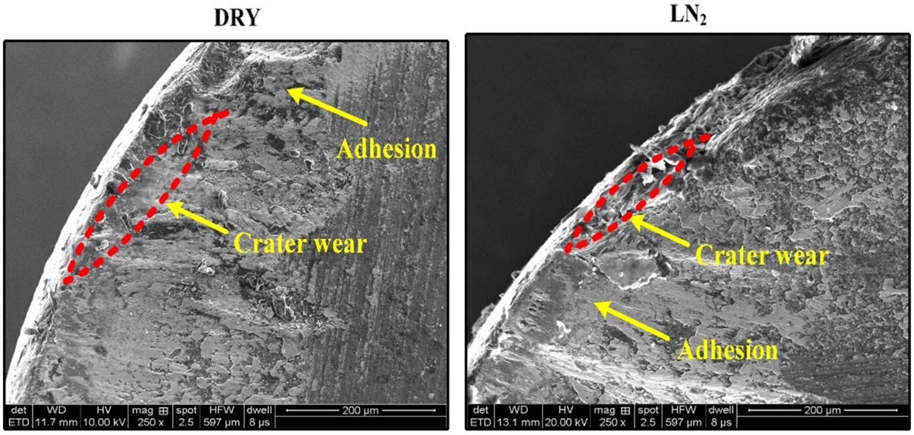

(a) *Vc* = *250 m/min*

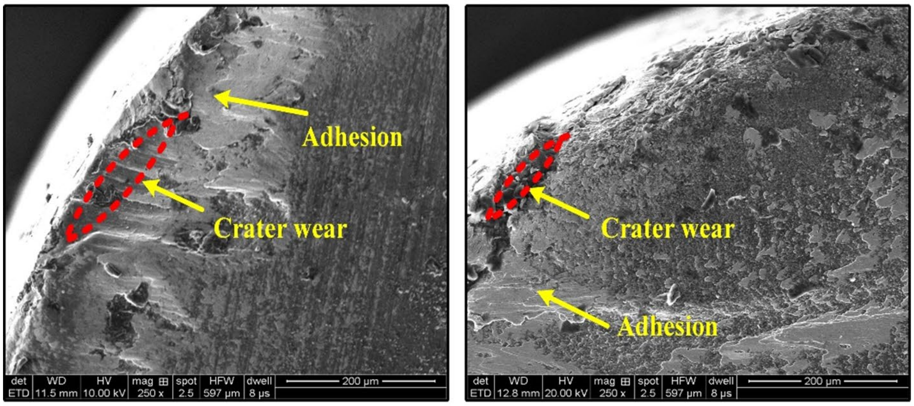

(b) *Vc* = *300 m/min*

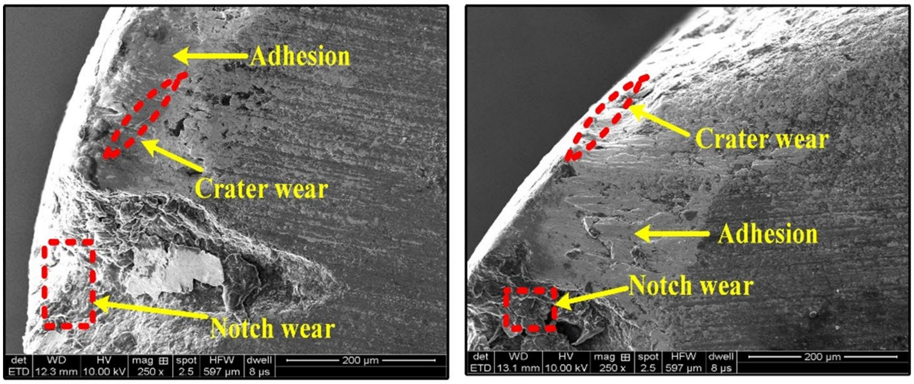

(c) *Vc* = *350 m/min*

Fig. 11 SEM images of the rake face after the inserts reaching the tool life

4 Conclusions

The high-speed turning experiments were carried out on Inconel 718 alloy by using ceramic inserts under dry and LN_2 machining. For different machining parameter combinations, the cutting vibration, machined surface roughness, tool wear, and microtopography of the flank face and rake face were analyzed.

Compared with dry machining, the using of LN_2 significantly reduces the vibration acceleration, improves the quality of the machined surface, reduces the tool–chip interface temperature and the friction between the tool–chip interface, reduces the shear strength of the workpiece material and reduces tool wear consequently.

Both in dry and LN_2 machining, notch and flank wear are the predominant wear of the ceramic inserts. The use of

LN_2 significantly improves the tool wear in terms of flank and notch wear compared with dry machining. This is due to the cushioning effect of LN_2 coolant and the reduction of the cutting temperature at the tool–chip interface.

Tool wear is the most important factor limiting the high-speed and high-precision machining of difficult-to-machine materials, such as Inconel 718 alloy. Many studies are worth pursuing further, such as new tool design, new cooling technique, cutting parameter optimization, and so on.

Acknowledgments This work is supported by the Special Fund of High-end CNC Machine Tools and Basic Manufacturing Equipment (2017ZX04002001), China.

References

1. Jafarian F, Umbrello D, Golpayegani S, Darake Z (2016) Experimental investigation to optimize tool life and surface roughness in Inconel 718 machining. Mater Manuf Process 31(13):1683–1691
2. Chetan Ghosh S, Rao PV (2016) Environment friendly machining of Ni–Cr–Co based super alloy using different sustainable techniques. Mater Manuf Process 31(7):852–859
3. Zhu D, Zhang X, Ding H (2013) Tool wear characteristics in machining of nickel-based super alloys. Int J Mach Tools Manuf 64:60–77
4. Paul S, Dhar NR, Chattopadhyay AB (2001) Beneficial effects of cryogenic cooling over dry and wet machining on tool wear and surface finish in turning AISI 1060 steel. J Mater Process Tech 116(1):44–48
5. Dhar NR, Paul S, Chattopadhyay AB (2002) Machining of AISI 4140 steel under cryogenic cooling–tool wear, surface roughness and dimensional deviation. J Mater Process Tech 123(3):483–489
6. Hong SY (2006) Lubrication mechanisms of LN2 in ecological cryogenic machining. Mach Sci Technol 10(1):133–155
7. Hong SY, Ding Y (2001) Cooling approaches and cutting temperatures in cryogenic machining of Ti-6Al-4V. Int J Mach Tools Manuf 41(10):1417–1437
8. Kaynak Y (2014) Evaluation of machining performance in cryogenic machining of Inconel 718 and comparison with dry and MQL machining. Int J Adv Manuf Tech 72(5–8):919–933
9. Venugopal KA, Paul S, Chattopadhyay AB (2007) Tool wear in cryogenic turning of Ti-6Al-4V alloy. Cryogenics 47(1):12–18
10. Dhananchezian M, Kumar MP, Sornakumar T (2011) Cryogenic turning of AISI 304 stainless steel with modified tungsten carbide tool inserts. Mater Manuf Process 26(5):781–785
11. Dhar NR, Kamruzzaman M (2007) Cutting temperature, tool wear, surface roughness and dimensional deviation in turning AISI-4037 steel under cryogenic condition. Int J Mach Tools Manuf 47(5):754–759
12. Al-Zaharnah IT (2006) Suppressing vibrations of machining processes in both feed and radial directions using an optimal control strategy: the case of interrupted cutting. J Mater Process Technol 172(2):305–310
13. Thomas M, Beauchamp Y (2003) Statistical investigation of modal parameters of cutting tools in dry turning. Int J Mach Tools Manuf 43(11):1093–1106
14. Devillez A, Dudzinski D (2007) Tool vibration detection with eddy current sensors in machining process and computation of stability lobes using fuzzy classifiers. Mech Syst Signal Process 21:441–456
15. Hessainia Z, Belbah A, Yallese MA, Mabrouki T, Rigal JF (2013) On the prediction of surface roughness in the hard turning based on cutting parameters and tool vibrations. Measurement 46(5):1671–1681
16. Abouelatta OB, Mádl J (2001) Surface roughness prediction based on cutting parameters and tool vibrations in turning operations. J Mater Process Technol 118:269–277
17. Richards N, Aspinwall D (1989) Use of ceramic tools for machining nickel based alloys. Int J Mach Tools Manuf 29:575–588
18. Kono Y, Hara A, Yazu S, Uchida T, Mori Y (1980) Cutting performance of sintered CBN tools. In: Proceedings of international conference on cutting tool materials. Fort Mitchell, KY, pp 281–95
19. Ezugwu EO, Pashby IR (1992) High speed milling of nickel-based superalloys. J Mater Process Technol 3:429–437
20. Ezugwu EO, Tang SH (1995) Surface abuse when machining cast iron (G-17) and nickel-base superalloy (Inconel 718) with ceramic tools. J Mater Process Technol 55:63–69
21. Narutaki N, Yamane Y, Hayashi K, Kitagawa T (1993) High speed machining of Inconel 718 with ceramic tools. Ann CIRP 42(1):103–106
22. Altin A, Nalbant M, Taskesen A (2007) The effects of cutting speed on tool wear and tool life when machining Inconel 718 with ceramic tools. Mater Des 28:2518–2522
23. Wanga Qiang, Wub Yongbo, Guc Jia, Lud Dong, Jie Yuebo, Nomurab Mitsuyoshi (2016) Fundamental machining characteristics of the in-base-plane ultrasonic elliptical vibration assisted turning of Inconel 718. Procedia CIRP 42:858–862
24. Akıncıoğlu Sıtkı, Gökkaya Hasan, Uygur İlyas (2016) The effects of cryogenic-treated carbide tools on tool wear and surface roughness of turning of Hastelloy C22 based on Taguchi method. Int J Adv Manuf Technol 82(1–4):303–314
25. Yıldırım Çagrı Vakkas, Kıvak Turgay, Erzincanlı Fehmi (2014) Tool wear and surface roughness analysis in milling with ceramic tools of Waspaloy: a comparison of machining performance with different cooling methods. J Braz Soc Mech Sci Eng 41(2):83
26. VakkasYıldırım Çağrı, Kıvak Turgay, Sarıkaya Murat, Şirin Şenol (2020) Evaluation of tool wear, surface roughness/topography and chip morphology when machining of Ni-based alloy 625 under MQL, cryogenic cooling and CryoMQL. J Mater Res Technol 9(2):2079–2092
27. Sivaiah P, Chakradhar D (2017) Influence of cryogenic coolant on turning performance characteristics: a comparison with wet machining. Mater Manuf Process 32(13):1475–1485
28. Carou D, Rubio EM, Lauro CH, Davim JP (2016) The effect of minimum quantity lubrication in the intermittent turning of magnesium based on vibration signals. Measurement 94:338–343
29. Sofuoglu Mehmet Alper, Orak Sezan (2015) A hybrid decision making approach to prevent chatter vibrations. Appl Soft Comput 37:180–195
30. Prasad BS, Babu MP (2017) Correlation between vibration amplitude and tool wear in turning: numerical and experimental analysis. Eng Sci Technol Int J 20(1):197–211
31. He CL, Zong WJ, Zhang JJ (2018) Influencing factors and theoretical modeling methods of surface roughness in turning process: state-of-the-art. Int J Mach Tools Manuf 129:15–26
32. Altin Abdullah (2014) Optimization of the turning parameters for the cutting forces in the hastelloy X Superalloy based on the Taguchi method. Mater Technol 48(2):249
33. Hessainia Z, Belbah A, Yallese MA, Mabrouki T, Rigal JF (2013) On the prediction of surface roughness in the hard turning based on cutting parameters and tool vibration. Measurement 46:1671–1681

34. Hong SY, Ding Y, Jeong WC (2001) Friction and cutting forces in cryogenic machining of Ti-6Al-4 V. Int J Mach Tools Manuf 41(15):2271–2285
35. Özbek NA, Çiçek A, Gülesin M, Özbek O (2016) Effect of cutting conditions on wear performance of cryogenically treated tungsten carbide inserts in dry turning of stainless steel. Tribol Int 94:223–233
36. Musfirah AH, Ghani JA, Che Haron CH (2017) Tool wear and surface integrity of Inconel 718 in dry and cryogenic coolant at high cutting speed. Wear 376–377:125–133
37. VakkasYıldırım Çağrı (2020) Investigation of hard turning performance of eco-friendly cooling strategies: cryogenic cooling and nanofluid based MQL. Tribol Int 144:106127
38. Ravi S, Kumar MP (2011) Experimental investigations on cryogenic cooling by liquid nitrogen in the end milling of hardened steel. Cryogenics 51(9):509–515
39. Gill SS, Singh H, Singh R, Singh J (2011) Flank wear and machining performance of cryogenically treated tungsten carbide inserts. Mater Manuf Process 26(11):1430–1441
40. Mozammel Mia Md, Khan Awal, Dhar Nikhil Ranjan (2017) Study of surface roughness and cutting forces using ANN, RSM, and ANOVA in turning of Ti-6Al-4V under cryogenic jets applied at flank and rake faces of coated WC tool. Int J Adv Manuf Technol 93:975–991
41. Ghani JA, Choudhury IA, Masjuki HH (2004) Performance of P10 TiN coated carbide tools when end milling AISI H13 tool steel high cutting speed. J Mater Process Technol 153:1062–1066
42. Akhtar W, Sun J, Chen W (2016) Effect of machining parameters on surface integrity in high speed milling of super alloy GH4169/Inconel 718. Mater Manuf Process 31(5):620–627
43. Zhuang k, Zhu D, Zhang X, Ding H (2014) Notch wear prediction model in turning of Inconel 718 with ceramic tools considering the influence of work hardened layer. Wear 313(1–2):63–74